Available online at www.sciencedirect.com
ScienceDirect
Catalysis Today 131 (2008) 118–124
CATALYSIS TODAY
www.elsevier.com/locate/cattod

Comparative study of Cu/ZnO catalysts derived from different precursors as a function of aging

E.N. Muhamad [a], R. Irmawati [a,*], Y.H. Taufiq-Yap [a], A.H. Abdullah [a], B.L. Kniep [b], F. Girgsdies [b], T. Ressler [b]

[a] *Department of Chemistry, Faculty of Science, Universiti Putra Malaysia, 43400 UPM Serdang, Selangor, Malaysia*
[b] *Department of Inorganic Chemistry, Fritz-Haber-Institute der MPG, Faradayweg 4-6, 14915 Berlin, Germany*

Available online 26 November 2007

Abstract

Structural modifications of Cu/ZnO catalysts for methanol steam reforming (MSR) as a function of precipitate aging in catalysts preparation process has been investigated comparatively. Freshly precipitated Cu,Zn-hydroxycarbonate (HC) and Cu,Zn-hydroxynitrate (HN) were aged in their mother liquor for a period of 120 min followed by washing, drying, calcination and reduction. Pronounced effect of aging was found for aged HC precipitates while no significant effect of aging was observed for aged HN solids. The bulk structure of the Cu/ZnO catalysts was investigated by means of TG/MS, *in situ* XRD and ^{63}Cu NMR. The increase in the activity of the catalysts prepared by HC aging did not correlate linearly with the specific Cu surface area but coincides with an increase in the microstrain in the copper clusters presumably because of the improved interface between Cu and ZnO. Meanwhile, aging of HN precipitates results in large, separated and less strained Cu and ZnO particles with an inferior catalytic activity. Finally, both aged Cu/ZnO catalysts revealed smaller copper crystallite size compared to unaged samples.

Keywords: Precipitating agent; Aging; Copper; Zinc oxide; Microstrain

1. Introduction

Cu/ZnO-based catalysts are well known industrial catalysts for the low temperature-pressure methanol synthesis [1,2], water-gas shift reaction [3] and hydrogenation of CO_x [4–7]. Recently, a lot of researches discussed its application for the production of hydrogen from methanol steam reforming and/or partial oxidation reaction especially for fuel cell application [5,6]. In spite of that many works have been carried out on in the applied and fundamental studies on Cu/ZnO catalysts, the focus has been mainly on improving the catalytic activity of Cu/ZnO-based catalysts by various modification techniques, i.e. addition of suitable promoter/support [8–10], combination with effective component [8,11,12] and implementation of new preparative method [13–15]. Nowadays however, many researchers have put their enthusiasm in tailoring the microstructural properties of Cu/ZnO catalysts without modifying the simple copper/zinc binary system. One of the attempts is to modify the bulk structure and induce structural disorder by aging process.

From literature survey, it is reported that in the production of commercial Cu/ZnO catalysts, a period of aging is essential [16]. During the aging process, the initial precipitate remains in contact with the precipitating agents, and the particles can partially redissolve or increase in size due to Ostwald ripening [17]. This particle growing phenomenon concerns only crystal of the same composition and structure (i.e. crystals of the same phase) which is in contrast with phase transition. In addition, phase composition is often reportedly changed during aging time [6,17]. The process of aging is found very often promoted by maintaining the precipitate and precipitation medium together at elevated temperatures for a period of time. Study by Li and Inui [18] on the effect of temperature and pH during precipitation of Cu/Zn/Al with sodium carbonate concluded that the optimum condition for the initial co-precipitation is at 343 K and at constant pH of 7. In their work they observed that despite the composition of the precursors obtained at pH 7 and temperature lower than 323 K was the same as those catalysts, which was obtained at pH 7 and temperature of 343 K, the catalytic activity of the former catalyst in methanol synthesis is

* Corresponding author. Tel.: +603 8946 6786; fax: +603 8946 6758.
E-mail address: irmawati@science.upm.edu.my (R. Irmawati).

0920-5861/$ – see front matter © 2007 Published by Elsevier B.V.
doi:10.1016/j.cattod.2007.10.010

much lower. Therefore, it seems that the pH value exerts its effect through altering the phase composition of the precursors, while the temperature does so through the precipitation kinetics of the precursors with same compositions [19].

Further study by other research groups reported that out of other precipitation parameters (i.e. precipitating agent, temperature, pH and additives), aging was stated to be an essential step to obtain catalysts of high activity and stability [20]. Whittle et al. [6] for instance have studied the performance of Cu/ZnO catalysts for CO oxidation. They found that the phase formation changes to a mixture of aurichalcite and rosasite by increasing aging time. The transformation consequently changed the morphology of the Cu/ZnO catalysts from needle-like/platelets to nanoparticles Cu/ZnO, which led to smaller crystallite size and high-surface area of the final catalysts. Another study by Waller et al. [21] showed that aging of the catalysts precursor obtained from mixed nitrate solution (Cu/Zn molar ratio 2:1) by precipitation at 333 K and pH 7 led to both smaller and better distributions of Cu and ZnO crystallites in the final catalysts.

Another interesting fact about aging is it promotes structural defect (i.e. microstrain). From this promotional effect, the activity of methanol synthesis can be directly correlated with the microstrain of copper per metal particles [22]. The defects in bulk structure may significantly enhance the catalytic activity of the catalysts. Further suggestion mentioned that the strain might be induced by metastable suboxide species penetrating the copper matrix [23]. The strong influence of strain on the adsorption properties of metal surfaces has already been shown in a number of experimental and theoretical studies [24]. Thus, aging permits improved catalysts performance by tailoring the preparation conditions instead of varying the chemical composition. Obviously this microstrain-activity relation is in contrast with previous assumption on that the activity of copper catalysts increases linearly with copper surface area.

In this study Cu/ZnO catalysts was synthesised through Cu/Zn-hydroxynitrate route and aging process was conducted. The physical and chemical properties of Cu/Zn-hydroxynitrate samples were investigated as comparison to former study done by other researchers at Fritz Haber Institute of Max-Planck Gesellschaft [22,25–27] who worked on Cu/Zn-hydroxycarbonate. Previous investigations on changes in the morphology of the copper catalysts obtained from aged precursors [22,25] lack details on the bulk structure-activity relationships. Therefore, this work attempts to elucidate and verify the effect of microstrain on the activity of Cu/ZnO catalysts. The resulting catalysts were then finally tested for methanol steam reforming (MSR) process.

2. Experimental

2.1. Catalysts preparation

The Cu/Zn-hydroxynitrate precursor for the Cu/ZnO catalysts (molar ratio of copper to zinc = 70:30) were prepared by precipitation of metal nitrate solutions with ammonium hydroxide at constant pH of 7. The reaction container was thermostated to 338 K. Two types of precipitates were prepared, i.e. unaged and aged precursors. For the effect of aging study, the resulting precipitates were aged in their mother liquor under continuous stirring for 120 min before recovered by filtration. The obtained blue greenish solids were then washed with deionized water (6× 170 ml) at ambient temperature and kept dried in oven at 393 K for 20 h. The solid powders were then calcined in static air at 603 K for 3 h (heating ramp = 6 K/min) and were denoted as *x*HN and *x*HC where *x* is aging time of 120 min, and HN and HC are hydroxynitrate and hydroxycarbonate, respectively. For unaged samples, they were identified as 0HN and 0HC, accordingly. The preparation of Cu/Zn-hydroxycarbonate precursors (molar ratio of copper to zinc = 70:30 at constant pH) was described in details in Ref. [27].

2.2. Catalysts characterization

The phase composition of the precursors has been determined by *ex situ* X-ray diffraction using a STOE STADI-P focusing monochromatic transmission diffractometer employing Cu Kα radiation, equipped with a Ge(1 1 1) monochromator, and a position sensitive detector (linear PSD) at ambient temperature. The samples were scanned in the 2θ range from 2° to 100° with a scanning rate of 0.001°/step. Meanwhile, *in situ* XRD measurements were conducted on a STOE Bragg–Brentano diffractometer (Cu Kα radiation, secondary Si monochromator, scintillation counter). About 25 mg of calcined CuO/ZnO precursors was reduced in 2 vol.% H_2/He at 523 K (heating ramp of 6 K/min) in an *in situ* cell equipped with a Bühler HDK S1 high temperature chamber [28]. For on stream reaction, the XRD patterns were recorded at 523 K under methanol steam reforming conditions in a 2θ range from 28.0° to 93.0° with a step width of 0.04° (counting time, 2 s/step). The microstructure analysis was done by software package WinXas 3.1 which is described in detail in Ref. [25]. The crystallite size calculations were done based on Scherrer's equation [28].

Thermogravimetric analysis was conducted during reduction on a NETZSCH STA 449 thermobalance under constant gas flow of 2 vol.% H_2 in helium at a total flow of 100 ml/min. Approximately 10 mg of each of the calcined precursors were heated in an Al_2O_3 crucible from 300 to 523 K at a heating rate of 6 K/min. For temperature programmed reduction (TPR) analysis, the dried precursors underwent calcination at 603 K in 21 vol.% O_2/He (heating ramp = 6 K/min) before being subjected to TPR. The evolution of the gas phase composition during calcination and reduction was monitored with a quadrupole mass spectrometer (Pfeiffer Omnistar).

Ex situ Cu NMR spectra of reduced Cu/ZnO catalysts were measured with a Bruker MSL 300 Spectrometer at 79.618 MHz for ^{63}Cu and 85.288 MHz for ^{65}Cu at 4.2 K in an Oxford cryostat. Spin-echo experiments (90–180°) were performed with a 90° pulse of 5.5 μs, a 'recycling delay' of 2 s, and a τ value of 25 μs. The ^{63}Cu NMR spectra shown were calibrated against CuBr (s) at −381 ppm [29]. Prior to the NMR measurements all reduced samples collected from fixed-bed reactor were carefully moved into Schlenk tube in a glove box to prevent exposure to air.

2.3. Catalytic activity

Catalytic activity of Cu/ZnO catalysts in methanol steam reforming reaction was performed in a fixed-bed flow reactor placed in an aluminium-heating block. About 10 mg sample diluted in 90 mg boron nitride was set in the reactor. The saturated reactant mixture of methanol and distilled water with a ratio of 1:1 was introduced to the reactor with a total flow of 44 ml/min at atmospheric pressure. The temperature was increased from 300 to 523 K at a ramp rate of 6 K/min. Evolution of gas phase composition was monitored with a mass spectrometer (Pfeiffer Omnistar). The methanol steam reforming activity (i.e. hydrogen production rate) was calculated under isothermal conditions (523 K) at steady state after ~30 min of reaction process.

3. Results and discussion

3.1. Precursors formation

The precipitation curves of two different precipitation processes are displayed in Fig. 1. The precipitation of Cu/Zn-nitrate with ammonium hydroxide as a function of aging shows no significant change in pH. The pH value of the solution remained constant at seven throughout the aging process. This is contradicts with the pH response gained in the precipitation of Cu/Zn-nitrate with sodium carbonate. In the later process, a sharp drop in pH value is observed approximately after 22 min of aging. After a while, the pH value returned back to its original level, but in a rather slow process until the aging process is stopped. It is believed that the pH drop observed is due to phase transformation of precipitates from an initial amorphous precursor, i.e. georgeite [$(Cu_2CO_3(OH)_2$] phase to crystalline phase of rosasite [$(Cu,Zn)_2CO_3(OH)_2$] and aurichalcite [$(Cu,Zn)_5(CO_3)_2(OH)_6$]. This transformation was detected by the XRD diffractogram of HC sample as reported by Bems et al. [27]. The crystallization of rosasite and aurichalcite coincides with the pH drop and this is a direct indicator for the transformation of the solid. As observed in the XRD, the positions of the reflections do not shift with aging and no further alteration of their shapes was observed after the drop point. This indicates that the crystal growth has stopped and the phase remained as mixture of crystalline rosasite and aurichalcite until the end of the aging time.

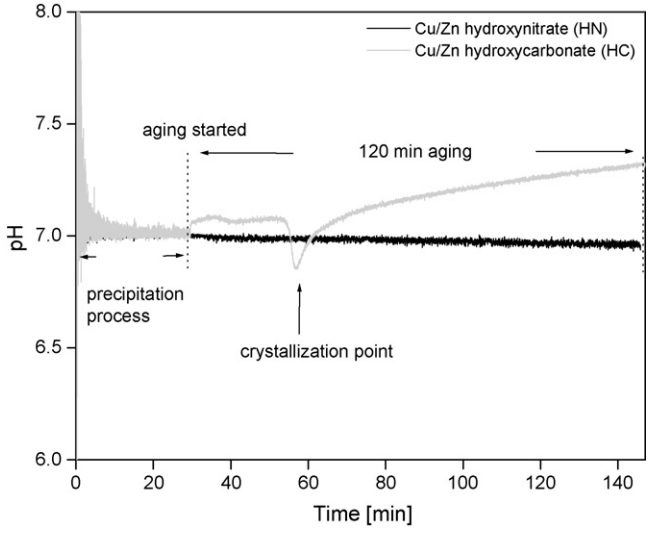

Fig. 1. pH curves of precipitation of Cu/Zn-nitrate with ammonium hydroxide (HN) and sodium carbonate (HC) as function of aging time at constant pH of 7.

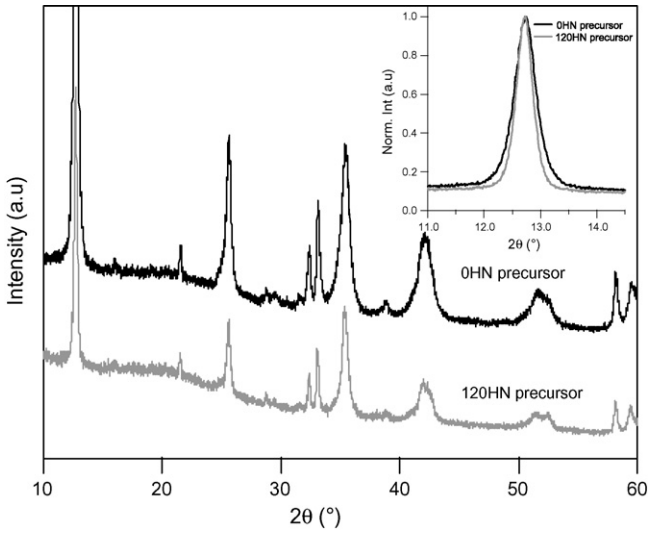

Fig. 2. X-ray diffractograms (XRD) of differently aged HN precursor and normalization intensity of most intense peak of gerhardite at $2\theta = 12.8^\circ$ (inset).

On the other hand, aging of the HN precursor in their mother liquor reveals no significant changes in pH signal. This indicates that there is no phase transformation or formation of other different phases, as evidenced in Fig. 2. By considering all the cations (Cu^{2+}, Zn^{2+}, NH_4^+) and anions (NO_3^-, OH^-) present in the samples, the resulting diffractogram of both HN precursors seems to be composed of one single phase that resembles gerhardite ($Cu_2(OH)_3NO_3$) [ICDD-PDF-2: 14–687] as evidenced by strong 002-reflection at $2\theta = 12.8^\circ$. Other reflections which correspond to the gerhardite phase are at $2\theta = 25.5^\circ$, 35.5°, 41.8° and 59.6°. However, some gerhardite peaks at 37.5° and 47.2° are missing and some unexplained peaks appear at $2\theta = 31.5^\circ$, 32.3° and 33.1°. While there is no zinc hydroxynitrate phase detected. This is in good agreement with the study by Sengupta et al. [30] in which they reported that precipitation of Cu/Zn-nitrate with ammonium hydroxide led to the formation of solid resembling gerhardite phase without the presence of zinc hydroxynitrate phase even by using as low as copper to zinc ratio of 30:70. On the occasion of deformed gerhardite structure, some zinc-containing samples can be assumed to incorporate in the gerhardite lattice. This sample gives gerhardite-like structure of the formula $(Cu,Zn)_x(OH)_3NO_3$. In the production of active catalyst, the formation of gerhardite phase must always be avoided during precipitation of Cu/ZnO catalyst system. This is because the formation and dispersion of active copper component depends to a great extent on the amount of gerhardite formed. The presence of gerhardite may cause sintering of copper oxide to occur which in turn makes the catalyst inactive [30].

Further observation of the HN samples was done by normalization of the most intense peak of the gerhardite-like phase at $2\theta = 12.8^\circ$ at the full width at half maximum (FWHM) of 0HN and 120HN precursors (Fig. 2, inset). It is shown that the 0HN precursor has wider peak compared to 120HN precursor. Thus the former sample has particle size smaller than the latter ones. The formation of bigger particle sized of aged sample is due to Ostwald ripening process.

3.2. CuO/ZnO

Thermal decomposition of precursor is analyzed in detail as it models the calcination steps in the catalyst synthesis. Combined thermal technique TG-DSC/MS was applied during calcination of HN precursors from 300 to 603 K in 21 vol.% O_2/He. Both samples exhibit similar decomposition and mass spectrometer profiles. Qualitative analysis of the mass loss curve reveals that all of the impurities decomposed in one single step as supported by sharp endothermic DSC signals as depicted in Fig. 3. The decomposition of HN precursors started approximately at 453 and 458 K for 0HN and 120HN samples, respectively. The small difference of approximately 5 K in the onset temperature of decomposition for both samples is probably due to the slightly large size particle of 120HN precursor coincides with a slightly slower response in the MS signal (not shown).

Fig. 4 shows the evolution of mainly H_2O (*m*/*z* 17 and *m*/*z* 18) and NO_x (*m*/*z* 30 and *m*/*z* 46) species. Small traces of NH_3 (*m*/*z* 15) and N_2O (*m*/*z* 44) are also detectable. This feature indicates the incorporation of additional phase during aging. Thus, decomposition of species was observed at different temperature. One significant reason for the growth of N_2O signal is the presence of ammonium nitrate (NH_4NO_3) phase. De Soete [31] reported that the decomposition of NH_4NO_3 can occur at 513 K to produce N_2O and H_2O. The decomposition of N_2O in the HN precursors here is most probably due to incomplete removal of NH_4NO_3 impurities during washing. Further decomposition of HN precursors was carried out up to

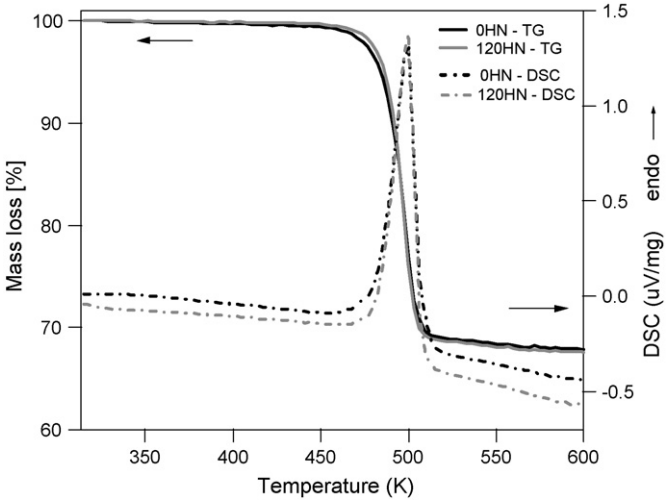

Fig. 3. TG/DSC signal during the calcination of 0HN and 120HN from 300 to 603 K (heating ramp of 6 K/min) under 21 vol.% O_2/He.

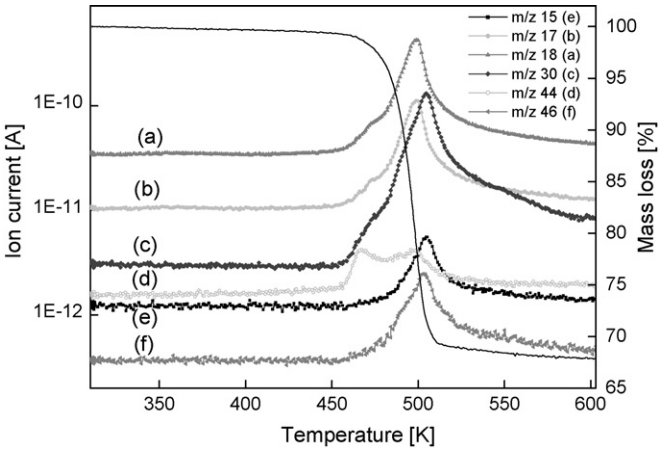

Fig. 4. Mass loss (TG) and the main mass fraction (MS) decomposed during the calcination of 0HN in 21 vol.% O_2/He (300–603 K, 6 K/min).

873 K to observe if any phase decomposes at higher temperature. The total weight loss calculated for both calcination temperatures is tabulated in Table 1. From the data given, it is found that the chosen calcination temperature (i.e. 603 K) is enough to eliminate all impurities in HN precursors to form CuO/ZnO.

On the other hand, decomposition of HC samples from 300 to 872 K reveals further decomposition at higher temperature [27,33]. Bems et al. reported that at high temperature range, i.e. from 713 to 753 K, the decomposition step is exclusively due to the release of CO_2. The decomposition of these carbonate species was referred as HT–CO_3. Since this species persists after the typical calcination temperature (603 K), thereby its presence may results in modification of microstructure of not only of the oxides but also of the reduced catalysts.

Calcination of 0HN precursor produces slightly bigger copper oxide crystallite compared to copper oxide particle obtained from calcined 120HN precursor. This occurrence could be due to more amount of gerhardite phase present in the precursor state of 0HN as shown by more weight loss by this sample during calcination (see Table 1). The presence of this phase consequently led to the formation of larger copper oxide due to severe sintering effect. This can be evidenced from the normalization of peak intensity of CuO[1 1 1] reflexes at $2\theta = 38.86^\circ$ (Fig. 5, inset). It shows that the crystallite size of CuO for aged sample is slightly smaller than the unaged CuO which is relative to the peak broadening (Fig. 5). The calculated CuO[1 1 1] crystallite size for 0HN is 214 Å and 200 Å for 120HN. Oh et al. [32] reported that the CuO prepared from ultrasonic spray pyrolysis have the particle size of 350 Å after underwent calcination at 673 K. Though the difference in HN samples is not so noticeable, aging process has been proven to produce smaller copper oxide particle compared to other techniques.

3.3. Reduction of CuO/ZnO

Fig. 6 shows the XRD diffractograms of Cu/ZnO. The patterns display characteristic peaks that matched perfectly

Table 1
Total mass loss during calcination at different temperatures from 300 to 603 K and from 300 to 873 K in 21 vol.% O_2/He (heating ramp of 6 K/min)

Calcination temperature (K)	Sample name	Mass of catalyst used		Weight loss experimental (wt.%)	Theoretical value (wt. %)
		Before (mg)	After (mg)		
603	0HN	8.601	5.791	32.67	33.71
	120HN	8.964	6.048	32.53	33.26
873	0HN	9.617	6.470	32.72	33.71
	120HN	14.87	10.110	32.01	33.26

with Cu [ICDD-PDF-2: 4–836] and ZnO [ICDD-PDF-2: 36–1451]. The main peaks for Cu at $2\theta = 43.3^\circ$, 50.4° and 74.1° correspond to [1 1 1], [2 0 0] and [2 2 0] crystal plane, respectively. The weight loss determined by TG analysis (14.94 wt.% for 0HN and 14.71 wt.% for 120HN) agrees well with the theoretical values of 14.63 wt.% for 0HN and 14.49 wt.% for 120HN. There is no Cu_2O or CuO present in the sample, which indicates all CuO, has been reduced to Cu metal. However, ZnO was not reduced under the same experimental conditions [10].

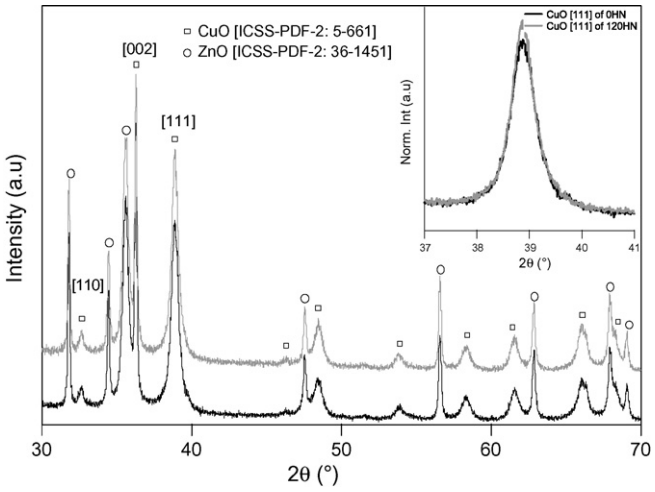

Fig. 5. X-ray diffractograms (XRD) of CuO/ZnO catalyst calcined in 21 vol.% O_2/He from 300 to 603 K prepared from HN samples. CuO[1 1 1] reflexes indicate smaller peak broadening of unaged CuO (0HN) (inset).

The reduction profile of Cu/ZnO catalysts derived from HN and HC is depicted in Fig. 7. The onset temperature of reduction of CuO/ZnO for HN samples started at 475 (120HN) and 479 K (0HN) and the reduction was completed approximately in 24 and 25 min, respectively. Whereas the TPR profile of HC samples shows a shift in onset reduction temperature from 462 (0HC) to 444 K (120HC). Kniep et al. [25] reported that differences in the onset of reduction temperature are due to the particle size effect where the copper crystallite size was 110 Å for 0HC and 70 Å for 120HC. The same trend was observed for HN sample. The Cu crystallite size calculated using Scherrer formula at the respective Cu[1 1 1] reflections revealed that the aged sample, 120HN has a Cu crystallite size of 236 Å compared to unaged sample 0HN with a crystallite size of 275 Å. Thus, the small-sized Cu particle is correlated to be an induction factor for the reduction process.

In situ X-ray diffraction enables the determination of microstructural characteristic of Cu/ZnO catalysts by analyzing the line profile of the X-ray diffraction peak. A sum of Pseudo Voigt functions and appropriate background function were refined according to Pawley method (''full pattern refinement'') to calculate the microstrain and Cu crystallite size (discussed in details in Ref. [25]). Fig. 8 shows the microstrain value of Cu at

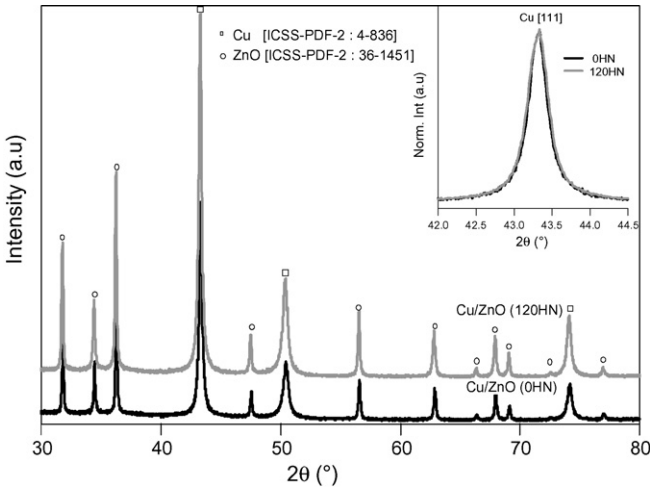

Fig. 6. X-ray diffractograms (XRD) of Cu/ZnO catalyst prepared from unaged (0HN) and aged (120HN) Cu,Zn-hydroxynitrate and the normalization of Cu[1 1 1] reflexes respective to Cu crystallite size (inset).

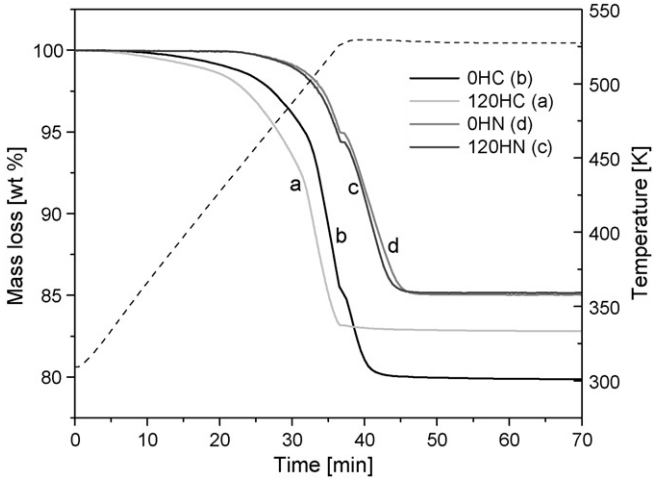

Fig. 7. Mass loss (wt.%) of HN and HC precursors during reduction (523 K; 6 K/min; 2% H_2/He). Earlier onset of HC reduction is due to particle size effect.

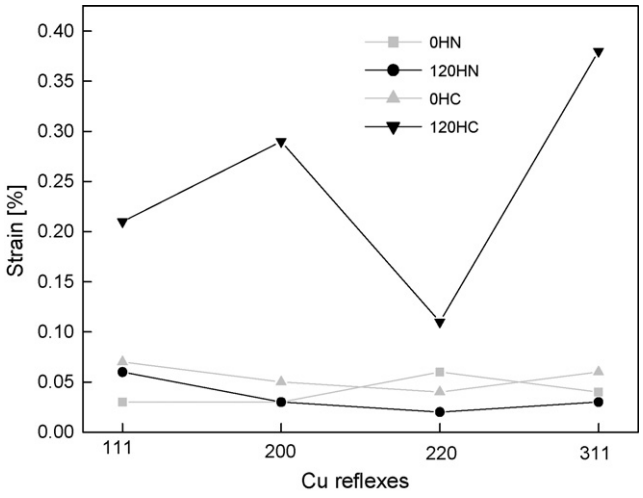

Fig. 8. Microstrain of Cu[111, 200, 220, 311] reflexes measured at 523 K during reduction in 2 vol.% H_2/He for 0HN, 120HN, 0HC and 120HC.

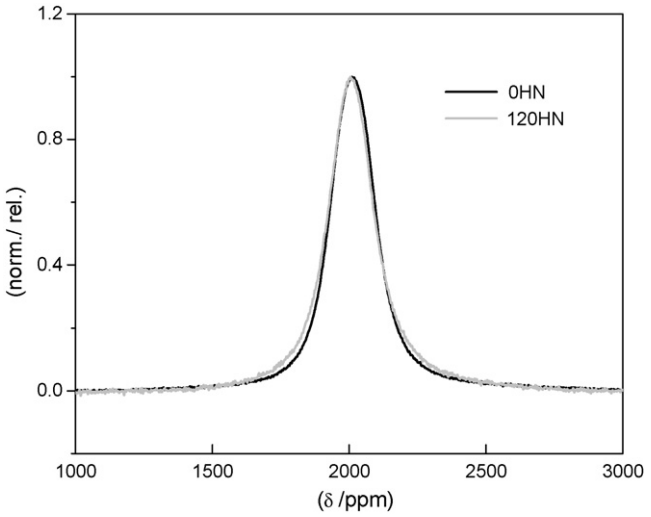

Fig. 9. Normalized ^{63}Cu NMR spectra of differently aged Cu/ZnO catalysts of 0HN and 120HN measured at 4.2 K (I_{rel} = intensity).

reflections [111, 200, 220, 311]. From the figure, the strain effect on copper can be divided into two groups. Based on Cu[1 1 1] reflections, high microstrain (0.22%) is detected for 120 min aging of HC, while low strain effect (∼0.03–0.07%) is detected for 0HN, 120HN and 0HC. These results clearly show that aging process has pronounced effect on the microstructural changes of copper, especially of aged HC sample.

To corroborate the data derived from X-ray diffraction experiment, *ex situ* ^{63}Cu NMR analysis was performed. Similar to X-ray diffraction line broadening, the line profile and breadth of the ^{63}Cu NMR signal is determined by the crystallite size and microstrain of the copper particles [28]. Large and highly ordered copper crystallites result in small and symmetric NMR signal. A decreasing copper crystallite size led to symmetric broadening of the NMR signal, whereas an increasing microstrain (disorder of the copper) results in asymmetric signal profiles or even additional NMR signals. The ^{63}Cu NMR spectra of differently aged Cu/ZnO catalysts for HN samples are shown in Fig. 9. The NMR spectra of the Cu/ZnO catalysts are in good agreement with the X-ray diffraction pattern. The peak profile of 0HN and 120HN shows that large and ordered Cu crystallite was formed which is close to ideal copper. Meanwhile, the ^{63}Cu NMR analysis for HC samples shows that highly structural disorder (i.e. microstrain) of copper particle, evidenced by asymmetric line broadening was observed for aged HC sample as described in detail in Ref. [26].

3.4. Catalytic methanol steam reforming reaction

The catalytic performances of the Cu/ZnO catalysts tested for H_2 production from methanol steam reforming are summarized in Table 2. There are huge differences in the catalytic activity of HN and HC samples as displayed in Fig. 10. The H_2 production rate of HC sample increases about 15% by prolonging aging time. Meanwhile at lower methanol conversion the activity of Cu/ZnO catalysts prepared from HN precursor increase about 6% from 45.7 (0HN) to 48.6 μmol/g s (120HN). From the catalytic study of Cu/ZnO catalysts in methanol steam reforming both aged samples (120HN and 120HC) show higher production rate of H_2 compared to non-aged ones (0HN and 0HC).

In addition to the activity of Cu/ZnO catalysts derived from HN and HC samples, the reaction was also carried out for unsupported copper catalysts obtained from malachite precursor [$Cu_2(OH)_2CO_3$] which has a particle size of 300 Å and a microstrain of 0.06% [26]. The catalytic activity data tabulated in Table 2 shows that even though the experimentally determined copper crystallite size of these three catalysts (i.e. 0HN, 120HN and malachite) is more or less similar, the HN samples were found to be more active than the unsupported copper catalysts. The small degree of strain in the unsupported copper material clearly demonstrates that the role of ZnO is not only to disperse copper [34] and prevent copper from sintering [1], but also influences the active species located on the Cu–

Table 2
Comparison in catalytic activity produced by differently prepared precursors under methanol steam reforming (MSR) condition at 523 K

Sample name	Cu[111] (Å)	Methanol conversion (%)	H_2 production rate (μmol/g s)	CO_2 production rate (μmol/g s)
0HN	275	22.3	45.7	17.6
0HC	110	75.2	139.9	52.6
120HN	236	26.7	48.6	17.5
120HC	70	82.2	161.1	63.9
Malachite	300	13.9	29.5	10.6

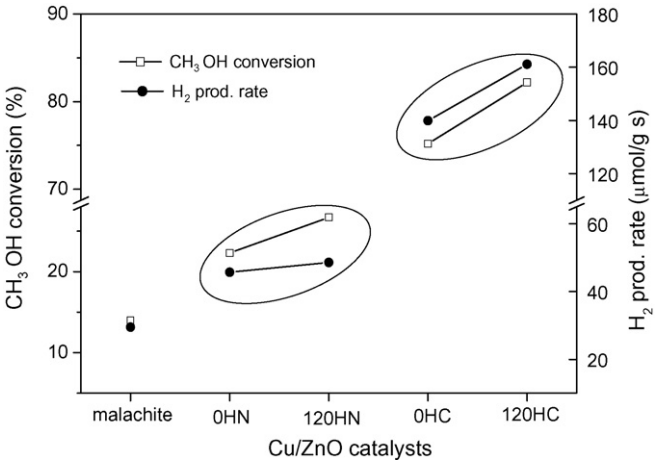

Fig. 10. H_2 production rate and CH_3OH conversion as a function of aging for differently prepared precursor (i.e. 0HN, 120HN, 0HC, 120HC, and malachite) of Cu/ZnO catalysts.

ZnO interface [35] where the spillover of hydrogen between Cu and ZnO occurs.

4. Conclusions

The characteristics phase transformation evidenced during aging of hydroxycarbonate was not observed in the precipitation of hydroxynitrate. Thus, precipitation using ammonium hydroxide led to the formation of a single phase precursor (HN) whereas using sodium carbonate resulted in a mixture of several Cu,Zn-hydroxycarbonates (HC). Aging of HN seems to have no clear effect in the phase composition other than the particle growth of the single phase that resembles gerhardite. The presence of gerhardite was believed to exert adverse effect for production of active Cu catalyst by forming larger copper particle (i.e. sintering effect). Carbonate species that were present in the Cu,Zn-hydroxycarbonate were assumed to be crucial in making active Cu/ZnO catalyst. Despite of phase composition, homogeneity and smaller crystallite size, high microstrain of copper particle prepared from HC is the main factor, which led to active Cu/ZnO catalyst compared to HN.

Assuming that copper microstrain originates from an epitaxial orientation of copper and zinc, the appropriate period of aging is essential to induce microstructural defect (i.e. microstrain) in copper particle to govern the properties of final desired catalyst. The higher strain amount of the catalysts prepared by 120 min aging of hydroxycarbonate (120HC) clearly indicates that the nanostructure character of the catalysts and the resulting distinct interfacial contact of ZnO to copper were necessary to prepare strained copper particles. The degree of the microstrain in copper clusters can be neglected for the non-supported system ($Cu_2(OH)_2CO_3$), the HN prepared catalysts (i.e. 0HN and 120HN) and the non-aged HC catalysts (0HC). Therefore in this study it can be clearly stated that a more defect-rich character (i.e. microstrain) of the copper particle and high interfacial contact between Cu and ZnO were necessary for an active catalyst.

Acknowledgments

The authors acknowledge the Malaysian Ministry of Science, Technology and Innovation (MOSTI) under 03-02-02-3010 SR0002/05-05 project for financial support. Technical assistance from Geometric Structure Group at FHI of MPG, Berlin, is gratefully acknowledged.

References

[1] G.C. Chinchen, P.J. Denny, J.R. Jennings, M.S. Spencer, K.C. Waugh, Appl. Catal. 36 (1986) 1.
[2] K. Klier, Adv. Catal. 31 (1982) 243.
[3] F.S. Stone, D. Waller, Top. Catal. 22 (2003) 305.
[4] G.R. Sheffer, T.S. King, J. Catal. 115 (1989) 376.
[5] S.H. Taylor, G.J. Hutchings, A.A. Mirzaei, Chem. Commun. 15 (1999) 1373.
[6] D.M. Whittle, A.A. Mirzaei, J.S.J. Hargreaves, R.W. Joyner, C.J. Kiely, S.H. Taylor, G.J. Hutchings, Phys. Chem. Chem. Phys. 4 (2002) 5915.
[7] Y. Ma, Q. Sun, D. Wu, W.H. Fan, Y.L. Zhang, J.F. Deng, Appl. Catal. A 171 (1998) 45.
[8] J.B. Breen, J.R.H. Ross, Catal. Today 511 (1999) 521.
[9] H. Kobayashi, N. Takezawa, C. Minochi, Chem. Lett. 12 (1976) 1347.
[10] G. Fierro, M. Lo Jacono, M. Inversi, P. Porta, F. Cioci, R. Lavecchia, Appl. Catal. A 137 (1996) 327.
[11] S. Velu, K. Suzuki, T. Osaki, Chem. Commun. (1999) 2341.
[12] G. Shen, S. Fujita, S.N. Matsumoto, Takezawa, J. Mol. Catal. A 124 (1997) 123.
[13] J.P. Shen, C. Song, Catal. Today 77 (2002) 89.
[14] M. Kurtz, N. Bauer, C. Büscher, H. Wilmer, O. Hinrichen, R. Becker, S. Rabe, K. Merz, M. Driess, R.A. Fischer, M. Muhler, Catal. Lett. 92 (2004) 49.
[15] H.L. Castricum, H. Bakker, E.K. Poels, Mater. Sci. Eng. A 304–306 (2001) 418.
[16] J. Agrell, B. Lindström, L. Pettersson, S.G. Järås, Catalysis 16 (2002) 67.
[17] R. Boistelle, J.P. Astier, J. Cryst. Growth 90 (1988) 14.
[18] J.L. Li, T. Inui, Appl. Catal. A 137 (1996) 105.
[19] M.S. Spencer, Top. Catal. 8 (1999) 259.
[20] F. Schüth, K. Unger, in: G. Ertl, H. Knözinger, J. Weitkamp (Eds.), Handbook of Heterogeneous Catalysis, vol. 1, VCH Verlagsgesellschaft, Weinheim, 1997, p. 72.
[21] D. Waller, D. Stirling, F.S. Stone, M.S. Spencer, Faraday Discuss. Chem. Soc. 87 (1989) 107.
[22] M.M. Günter, T. Ressler, B. Bems, C. Büscher, T. Genger, O. Hinrichsen, M. Muhler, R. Schlögl, Catal. Lett. 71 (2001) 37.
[23] A. Knop-Gericke, M. Hävecker, T. Shedel-Niedrig, R. Schlögl, Top. Catal. 15 (2001) 27.
[24] S. Sakong, A. Grob, J. Catal. 231 (2005) 420.
[25] B.L. Kniep, F. Girgsdies, T. Ressler, R. Schlögl, J. Catal. 236 (2005) 34.
[26] B.L. Kniep, T. Ressler, A. Rabis, F. Girgsdies, M. Beanitz, F. Steglich, R. Schlögl, Angew. Chem. Int. Ed. 43 (2004) 112–115.
[27] B. Bems, M. Schur, A. Dassenoy, H. Junkes, D. Herein, R. Schlögl, Chem. A: Eur. J. 9 (2003) 2039.
[28] A. Szizybalski, F. Girgsdies, A. Rabis, Y. Wang, M. Niederberger, T. Ressler, J. Catal. 233 (2005) 297.
[29] J. Mason, Multinuclear NMR, Plenum Press, New York, 1989.
[30] G. Sengupta, D.P. Das, M.L. Kundu, S. Dutta, S.K. Roy, R.N. Sahay, K.K. Mishira, Appl. Catal. 55 (1989) 165.
[31] G.G. De Soete, Oil Gas Sci. Tech. 45 (1990) 663.
[32] S.W. Oh, H.J. Bang, Y.C. Bae, Y.K. Sun, J. Power Sources 173 (2007) 502.
[33] M.J.L. Ginés, C.R. Apesteguía, J. Thermal Anal. 50 (1997) 745.
[34] R. Burch, S.E. Golunski, M.S. Spencer, J. Chem. Soc., Faraday Trans. 86 (1990) 2683.
[35] Z. Wang, W. Wang, G. Lu, Int. J. Hydrogen Energy 28 (2003) 151.